

See discussions, stats, and author profiles for this publication at: <https://www.researchgate.net/publication/231372846>

Importance of Proton Conductivity Measurement in Polymer Electrolyte Membrane for Fuel Cell Application

ARTICLE *in* INDUSTRIAL & ENGINEERING CHEMISTRY RESEARCH · MAY 2005

Impact Factor: 2.59 · DOI: 10.1021/ie0501172

CITATIONS

132

READS

286

4 AUTHORS, INCLUDING:



Chang Hyun Lee

Seoul National University Hospital

157 PUBLICATIONS 2,768 CITATIONS

SEE PROFILE



Ho Bum Park

Hanyang University

106 PUBLICATIONS 4,238 CITATIONS

SEE PROFILE

Importance of Proton Conductivity Measurement in Polymer Electrolyte Membrane for Fuel Cell Application

Chang Hyun Lee,[†] Ho Bum Park,[†] Young Moo Lee,^{*,†} and Rae Duk Lee[‡]

School of Chemical Engineering, College of Engineering, Hanyang University, Seoul 133-791, Korea, and Division of Electromagnetic Metrology, Korea Research Institute of Standards and Science, Yuseong, Daejeon 305-600, Korea

The precise impedance measurement system based on the well-known two-probe and four-probe methods was prepared to measure the impedance and consequent proton conductivity of Nafion membranes as standard samples, considering not only the number of electrodes and the bridging methods but also the elimination of electrical error sources for the precise electrical analysis. The proton conductivities of Nafion membranes are reported and discussed in the present study with respect to different cell configurations and measurement conditions. The values of proton conductivities measured using the four-probe method were always higher (2–5 times) than those measured using the two-probe method at ambient humidity and temperature. The proton conductivities were also measured under two different humidity conditions: water-vapor state and liquid-water state. In the water-vapor state (95% relative humidity), completely different impedance behaviors for the identical Nafion membrane were observed from the Nyquist impedance plots. All Nyquist plots derived from the two-probe method represented the inductive reactance derived from various components, such as Pt electrodes, electric conductive leads, and a potentiometer in the path of current flow rather than the capacitive reactance between Pt electrodes. The effect of contact resistance between the membrane sample and electrodes on proton conductivity was also investigated by using the two conductivity-cell configurations. It was shown that the effect of the contact resistance on the proton conductivity was more severe in the two-probe measurement, and this factor should be seriously considered in the water-vapor state. Furthermore, the humidity and the temperature effects on the proton conductivity of the membranes were observed under various measuring conditions and compared with the two different cell configurations. The four-probe method well reflected the proton conductivity behavior of Nafion membrane in the wide range of temperature and humidity, as compared with the two-probe method with reasonable proton conductivity in the low humidity.

Introduction

In a cation-exchange membrane, the proton transports along with hydrated structures connected with negatively charged fixed ions (sulfonate ion, phosphate ion, and carboxylate ion groups, etc) or by aid of water molecules within the membrane. Actually, the proton transport mechanism is very complex, and the vehicle or hopping mechanism is a well-accepted hypothesis for the transport.^{1–7} Materials showing high proton conduction are in strong demand in the fuel cell field, one of the next-generation alternative energy sources. In particular, the polymer–electrolyte–membrane fuel cell (PEMFC) operates using fuels such as hydrogen and methanol at ambient temperature, and it needs highly proton conductive polymer membranes in order to obtain a high voltage per current density in the unit cell. Therefore, many researchers have focused on the development of highly proton conductive polymer membranes to achieve early commercialization of PEMFC. There are many prerequisite factors in the research and development of proton exchange membranes, but the accurate measurement of proton conductivity through the membrane is of prime significance.

For this purpose, several measurement methods^{8–22} have been suggested and used to obtain the proton conductivity using the voltage drop between electrodes. Although there has been a new attempt to measure proton mobility through the diffusivity of mobile hydrogen ions using pulsed field gradient spin–echo (PGSE) NMR, the proton transport behavior by the Gröthaus hopping mechanism, which is highly significant at high water content but negligible at low water content, was not well observed, compared with the diffusivity determined by estimation of the proton conductivity using the Nernst–Einstein equation.²³ In addition, the conductivity in the proton-conductive material with the previously described fixed charge anion groups in the hydrated state originates from only the mobile proton, as proton conductivity in deionized water is low enough (5.7×10^{-8} S/cm) at room temperature to be neglected in the conductivity contribution.²⁴

The proton conductivity is generally obtained from the measurement of resistivity of the proton-conductive membrane against the flow of either alternating current (ac) or direct current (dc). Despite the simplicity of the dc method, polarization, the distribution of chemical potential, and changes of electrode reaction should be considered in the measurement of resistivity with the current flow, which are classified into the two-terminal and four-terminal methods. The four-terminal method is usually used to measure the resistivity of ion conductors with low resistance, because of the reduced inter-

* To whom correspondence should be addressed. Tel.: +82-2-2220-0525. Fax: +82-2-2291-5982. E-mail: ymlee@hanyang.ac.kr.

[†] Hanyang University.

[‡] Korea Research Institute of Standards and Science.

facial resistance and polarization, whereas the two-terminal method is restrictively applicable to the measurement of resistivity in material of high resistance (above $10^6 \Omega$), as the contribution for resistance of the lead itself is low enough to be neglected in the total resistance. However, the four-terminal dc method should be never used for material with frequency-dependent behavior, such as being both an insulator and dielectric, despite the accuracy, the sensitivity, and the stability of the measurement.²⁵ Additionally, unfavorable ionic blocking is formed and subsequently results in inaccurate measurement when the proton conductivity is measured using irreversible electrodes in dc.

Therefore, the proton conductivity in a sample material with dielectric properties should be measured using the ac impedance spectroscopic technique. Despite the complexity in the interpretation of the spectroscopic diagram, the ac impedance method is more reasonable if the polarization and electrode reactions are eliminated. The impedance, which takes the phase difference into account, is a combined parameter for characterizing an electronic circuit; its components, such as resistors, inductors, and capacitors; and the component materials. The impedance (Z) is defined as the ratio of the voltage to the current at a given frequency, and it is represented as a complex quantity that consists of a real part (resistance, Z' or R) and an imaginary part (reactance, Z'' or $X_C - X_L$) with phase angle θ as described in eqs 1–3.

$$Z' = |Z| \cos \theta \quad (1)$$

$$Z'' = |Z| \sin \theta \quad (2)$$

$$\theta = \tan^{-1} \left(\frac{Z''}{Z'} \right) \quad (3)$$

The impedance can be expressed using the rectangular-coordinate form as $Z' + jZ''$ (Nyquist plot) or as the logarithm of the absolute magnitude of total impedance ($\log |Z|$) vs the logarithm of the angular frequency ($\log \omega$) (Bode plot).

In a practical electrochemical experiment, there are several methods for measuring the impedance, which have advantages and disadvantages depending on the intended use, the magnitude of the impedance, and the measuring conditions. Therefore, it is necessary to choose the most appropriate method by considering the frequency range, the measurement range, the measurement accuracy, and the simplicity of operation. Among the ac impedance measurement methods, the autobalancing bridge method is most favorable for general-purpose measurement because of its wide frequency range from 5 Hz to 40 MHz and its high accuracy over a wide impedance measurement range.²⁶ The autobalancing bridge is equipped with four coaxial terminals (current Lo, voltage Lo, current Hi, voltage Hi). The impedance is measured by recording the voltage drop between reference electrodes (voltage Hi, voltage Lo) while a constant current from the working electrode (current Hi) to counter electrode (current Lo) is imposed.

Although there are several connection modes used to interconnect a sample material using the autobalancing bridge method, the four-electrodes set with four-terminal connection (four-probe method) and the two-electrodes set with four-terminal connection (two-probe method) is generally used to measure the impedance of a sample material. The two interconnection methods differ with regard to the configuration of current-flowing

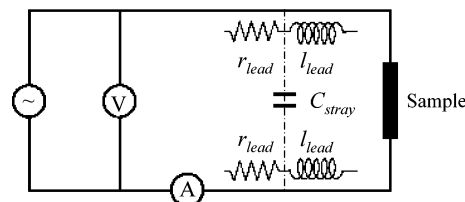


Figure 1. Schematic diagram of the two-probe method (V, voltmeter; A, ampere meter; C_o , stray capacitance between two leads; R_o , lead resistance; and L_o , lead inductance).

electrodes and voltage-sensing electrodes. In the two-probe method, the voltage drop is measured simultaneously across the same two electrodes as a constant current flows. In the four-probe method, two different pairs of electrodes are used; the outer pair to impose a constant current, and the inner pair to record the voltage drop as a response.

The two-probe method is a simple and convenient mode and has been used to measure total impedance of an electrochemical cell containing anode, cathode, electrolyte, and organic or inorganic fillers. However, the impedance in the two-probe method is obtained from the voltage drop to a constant current flow through the same electrodes. Accordingly, the impedance in the two-probe method reflects many impedance components, in the pathway that the current flows, such as the lead inductance (l_{lead}), the lead resistance (r_{lead}), and the stray capacitance (C_{stray}) between two leads, as shown in the simple electric circuit in Figure 1. In other words, the extra impedance derived from these impedance components is added to the measurement result including the impedance of sample materials. Because of the existence of these errors, the typical impedance measurement should be limitedly applied to sample materials only with the high impedance above 10 k Ω , where other impedance components with relatively low values can be disregarded.²⁶ On the contrary, the four-probe method can eliminate the effects of the lead impedance containing the l_{lead} , r_{lead} , and C_{stray} , because of the connection using four separate leads and no current on the leads for voltage sensing. Additionally, the measurement accuracy is improved not only in the high impedance measurement range but also in the low impedance range below 1 Ω .

In practice, many research groups have measured the impedance in proton-conductive materials, using either the four-probe method^{8–16} or the two-probe method.^{17–22} However, it seems that a standard measurement method for measuring exact proton conductivity has not been established yet. Furthermore, they considered only the number of electrodes and the bridging methods. However, the additional consideration to eliminate the effect of electrical error sources in the impedance measurement should be required for the precise electrochemical analysis. These error sources include the capacitance and the inductance between the leads, the stray capacitance between the leads, the contact resistance between the electrodes and the membrane sample, and the outer electromagnetic noise. Accordingly, inappropriate measurement methods containing electrical error sources can result in imprecise and different proton conductivities, even for the same material, which act as severe obstacles to the development of effective proton-exchange membranes with high performance. For this reason, it is very important to prepare the precise impedance measurement system and to disclose the more appropriate impedance measurement method

under a specific measurement condition similar to the practical fuel cell operating condition, through the comparison of proton conductivity from the four-probe method and the two-probe method using the measurement system in a wide humidity and temperature range.

Despite different methodologies, most research groups have used eq 4, which is generally applied to measure the ionic or electronic conductivity from the resistance of a sample material in dc, to obtain a proton conductivity (σ) of proton-exchange membrane materials with an impedance derived from the two-probe or the four-probe method.

$$\sigma = \frac{1}{R_s S} = \frac{l}{X} \quad (4)$$

where R_s is the bulk resistance of the membrane sample derived from an impedance analyzer, l is the distance between the reference electrodes, S is the cross sectional area of the membrane sample, i is the current density, and X is the electric field strength. X is defined as the ratio of the measured potential difference ($d\phi$) to the infinitesimal distance dx between the points of attachment to the voltmeter.

$$X = -\frac{d\phi}{dx} \quad (5)$$

Here, the bulk resistance consists of the ohmic resistance, the contact resistance, and the intrinsic resistance of the Pt electrode. It is considered that the bulk resistance is the ohmic resistance, because the contact resistance and the resistance of the Pt electrode are small enough to be negligible compared with the ohmic resistance.

The main objectives of this study is not to describe the proton conductivity of proton exchange membranes such as Nafion but to give more correct information on the measuring method for proton conductivity of the membranes. Nafion was just used in this study because it is a representative polymer that has been extensively investigated owing to its excellent proton conductivity. In this study, we prepared a precise impedance measurement system containing the electrode systems to measure and compare impedances in the membrane samples using both the two-probe and four-probe method in a thermo- and hygrocontrolled chamber. Especially, in the preparation of the measurement system, the usual copper leads are replaced with coaxial cables in order to minimize the stray capacitances and to shield the electromagnetic noise from outside of the sample. Even though the connection method using the usual copper leads has been widely used to measure dc resistivity, nobody reports on effectiveness by using coaxial cables for the ac resistivity or conductivity. The proton conductivity of Nafion 112, 115, and 117 as reference membrane samples was obtained using eq 4 via approximation of the impedance measured with the two methods at constant humidity and temperature. In addition, the effect of the contact resistance between the membrane samples and the electrodes on the proton conductivity was also investigated with different conductivity cell configurations.

Experimental Section

Materials. Nafion 112, 115, and 117 membranes were pretreated by boiling in deionized water for 1 h,

subsequently boiling in dilute H_2O_2 solution for 1 h to remove residual organic molecules, rinsing in boiling deionized water, boiling in 1 M sulfuric acid solution for 1 h to remove any possible inorganic contaminants, and finally rinsing in deionized water to neutral pH.

Measurement. The impedance of each proton exchange membrane as a proton conductor and dielectric was accurately determined using the electrode systems, which contained four different kinds of cells (a two-probe cell and a four-probe cell, for impedance measurement in water vapor, and a two-probe cell and a four-probe cell, for impedance measurement in liquid water), connected with an electrochemical interface (Solatron 1287) in combination with an impedance/gain-phase analyzer (Solatron 1260). The electrode systems were installed in the electrically shielded thermo- and hygrocontrolled metallic chamber. As shown in Figure 2a, the overall system for impedance measurement in the water-vapor state was composed of two parts: the base plate and the electrode system. In the base plate for the electrical connection, four BPO coaxial sockets with slots in the side of the socket were equipped to prevent any flooding by condensation of water vapor and were interconnected with a low-noise coaxial cable. The copper core in the low-noise coaxial cable was wrapped with Teflon insulator, aluminum coil, electrical shield net, and PVC insulator. The electrical shield net was interconnected with the base plate and the thermo- and hygrocontrolled metallic chamber to induce the complete electromagnetic shielding through the formation of a ground potential path. In the electrode system, four BPO plug connectors, which interconnected with Pt wire electrodes on a Teflon plate, were established to enable assembly and disassembly of the two-probe or the four-probe cell conveniently onto the base plate for electrical connection by way of plug-in and plug-out. Here, the use of BPO connectors and BPO coaxial sockets leads to the elimination of contact resistance between the base plate and the electrode system. A window was introduced to prevent condensation of water vapor at high relative humidity and to maintain the equilibrium state of the membrane with constant water content in situ. The membrane sample was fixed with six knurled nuts and a Teflon cover to maintain the same contact resistance by a constant torque of 0.5 kgf·cm for accurate impedance measurement. In addition to the base plate and the electrode system, a water reservoir, whose wall was coated with Teflon to avoid the formation of a short circuit, was set up to measure the impedance of the membrane sample in liquid water, as shown in Figure 2b. The whole structure was installed in a thermo- and hygrocontrolled metallic chamber that was electrically shielded to ensure a more stable measurement without any noise.

Maintaining a constant water content in the membrane is necessary for accurate impedance measurements, as the ion transport behavior through the membrane can be considerably affected, depending upon different hydration states. To maintain a more accurate water-vapor pressure for precise impedance measurements at constant humidity, a hygrometer connected with a humidity controller in a thermo- and hygrocontrolled chamber was previously calibrated by standard saturated salt solutions with well-known water activity. The humidity calibration in isopiestic equilibrium with relative humidity $11 \pm 1\%$, $33 \pm 1\%$, $53 \pm 1\%$, $75 \pm 1\%$, and $97 \pm 1\%$ at $25 \pm 1^\circ\text{C}$ was made by keeping the

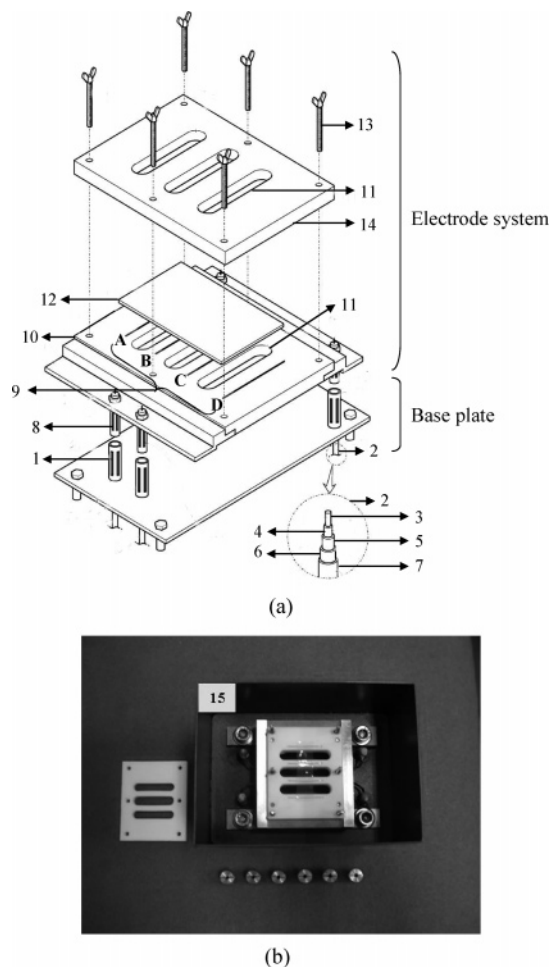


Figure 2. Schematic diagram of (a) the overall system for the impedance measurement in the water-vapor state. The base plate: 1, BPO coaxial sockets; 2, low-noise coaxial cable; 3, copper core; 4, Teflon insulator; 5, aluminum foil; 6, electrical shield net; 7, PVC insulator. The electrode system: 8, BPO plug connectors; 9, Pt wire electrodes [A electrode (working electrode, current I_i), B electrode (ref 2, voltage H_i), C electrode (ref 1, voltage L_o), and D electrode (counter electrode, current H_i). Each electrode is connected with corresponding BPO plug connector. In the case of the two-probe cell, the A electrode coincides with the B electrode at the B electrode site, and the D electrode coincides with the C electrode at the C electrode site.]; 10, Teflon plate; 11, a window to prevent condensation of water vapor and to maintain the equilibrium state of the membrane with constant water content in situ; 12, a membrane sample for measurement; 13, knurled nuts; 14, Teflon cover. Schematic diagram of (b) the electrode system for impedance measurement in the liquid-water state; 15, a water reservoir with Teflon-coated wall.

hygrometer connected with a humidity controller in a sealed container for 2 days; using saturated lithium chloride [LiCl], magnesium chloride [MgCl₂], magnesium nitrate [Mg(NO₃)₂], sodium chloride [NaCl], and potassium sulfate [K₂SO₄] solution, respectively;²⁷ and setting the equilibrium relative humidity up as a calibrated humidity. Using a similar procedure with saturated salt solutions, the hygrometer was calibrated within different temperature ranges.

Prior to impedance measurement under hygro- and thermocontrolled conditions, all Nafion membranes were dried at 105 °C under vacuum to produce the fully dehydrated state of membranes without any water uptake.²⁸ The impedance measurement was carried out, after each dried Nafion membrane introduced into the impedance measurement system was allowed to reach

equilibrium water content at a controlled humidity and temperature. A reduction of the impedance in proton-conductive membrane materials is generally observed as the temperature and the humidity increase. At equilibrium, the impedance of each Nafion membrane was continuously kept at a constant value after the rapid decrease or increase of the impedance under hygro- and thermocontrolled conditions. The impedance of each Nafion membrane was measured using the ac impedance spectroscopic techniques: the two-probe and four-probe method in the frequency range from 100 kHz to 0.1 Hz at a constant current of 1 mA. The impedance of the membrane sample at controlled humidity and temperature can be measured by way of a Nyquist plot and a Bode plot. For the Nyquist plot, both the real (Z') and imaginary parts (Z'') of the components of impedance in the membrane sample were simultaneously measured over a defined frequency range. When the imaginary component containing both the inductive reactance and the capacitive reactance approaches zero at higher frequency, the real Z' -axis intercept is close to the ohmic resistance and can be considered as the ohmic resistance of a membrane sample, eliminating any effect of the reactance caused by the lead inductance and the stray capacitance. For the Bode plot, the change of impedance is observed over a wide frequency range. The ohmic resistance of the sample is derived from the constant impedance within a reasonable frequency range, as compared with the approximation from the Nyquist plot. Finally, the proton conductivity is obtained by using eq 4 with a measured ohmic resistance, the spacing between the reference electrodes, and the cross-sectional area of the membrane sample.

The ratio of the mole number of water molecules to the fixed-charged sulfonate groups, which is denoted as λ , was obtained from the ion exchange capacity (IEC) via the conventional titration method (ASTM D 2187), and the water content (W) in the membrane at a specific humidity condition using a dynamic vapor sorption apparatus (DVS-1000, Surface Measurement System Ltd., London, UK), as described in eq 6

$$\lambda = \frac{W}{\text{IEC} \times 18 \text{ g/mol}} = \frac{(M_w - M_d)/M_d}{\text{equivalent} - \text{SO}_3\text{H}/M_d} \quad (6)$$

where M_w and M_d are the wet weight and the dry weight of a membrane sample, respectively.

Results and Discussion

The equilibrium of water sorbed in the Nafion membranes was set by a hygrometer calibrated with the saturated salt solution method, as described in Figure 3. To confirm the equilibrium water content of membrane samples under isothermal and isobaric conditions, repeated impedance measurements were carried out after hydration for 6 h to obtain the constant impedance at a fixed frequency. The measured impedance was used in eq 4 to obtain the proton conductivity of the sample. Equation 4, which is commonly used in dc measurements, can also be used in ac impedance spectroscopy, because the ohmic resistance of a sample is theoretically the same in both dc and ac. The approximated value at which reactive impedance $|X_C - X_L|$ in the following impedance measurement (eq 7) is so small as to be neglected, is expressed as the resistance (R) of the sample. In other words, the resistance is estimated and

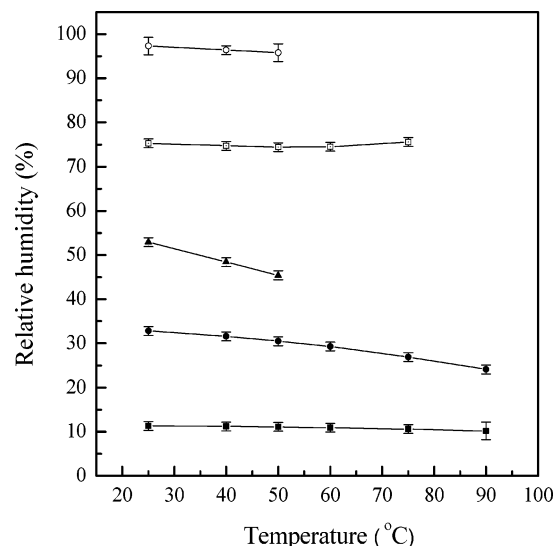


Figure 3. The equilibrium relative humidity of saturated solutions of inorganic salt, such as lithium chloride (LiCl, ■), magnesium chloride (MgCl₂, ●), magnesium nitrate (Mg(NO₃)₂, ▲), sodium chloride (NaCl, □), and potassium sulfate (K₂SO₄, ○) over a reasonable temperature range.

recorded as the impedance (Z) at the extrapolated intercept on the real axis of the impedance curve within a reasonable frequency range.

$$Z = \sqrt{R^2 + (X_C - X_L)^2} \quad (7)$$

$$\theta = \tan^{-1} \left(\frac{X_C - X_L}{R} \right) \quad (8)$$

where X_C and X_L are the capacitive reactance and the inductive reactance, respectively.

The impedance (Z) is frequency-dependent. Therefore, impedance spectroscopy using the Nyquist plot or the Bode plot shows the change in impedance over a reasonable frequency range and gives information on the electrochemical properties of proton-conductive membranes and the interface between the electrodes. The proton-conductive polymeric membrane has an electrochemical behavior similar to the electrical conductivity in a solid electrolyte, which is analyzed in terms of an equivalent circuit consisting of resistors and capacitors.²⁹ The Nyquist plot and the equivalent circuit for a simple parallel combination of a resistor with $R = 100 \, \Omega$ and a capacitor with $C = 1 \, \mu\text{F}$ is shown in Figure 4. Each impedance component in the parallel circuit makes a hemispheric Nyquist plot with the real part (Z') and the imaginary part (Z'') over different frequencies, as described with eq 9

$$Z = Z' - jZ'' = R - j(X_C - X_L) = \frac{R_p}{1 + \omega^2 C^2 R_p^2} - j \frac{\omega C R_p}{1 + \omega^2 C^2 R_p^2} \quad (9)$$

where R_p and C are the resistance and the capacitance in the parallel circuit, respectively.

The impedance measurement was performed using two different electrode configurations with Nafion 112, 115, and 117 under thermo- and hygrocontrolled conditions, such as 30–90 °C and 20% relative humidity (RH) to liquid water, respectively. As shown in Figure 5, the different impedance measurement methods in the water-vapor state led to a clearer difference in impedance

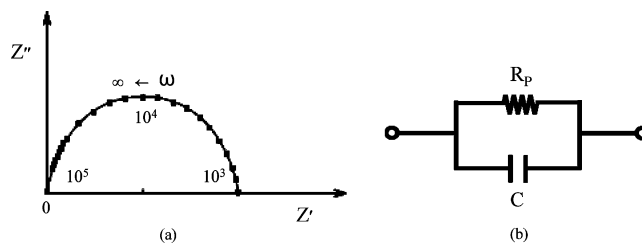


Figure 4. The simple equivalent circuit: (a) the Nyquist plot for a parallel RC circuit with $R_p = 100 \, \Omega$ and $C = 1 \, \mu\text{F}$ and (b) the equivalent circuit for the Nyquist plot.

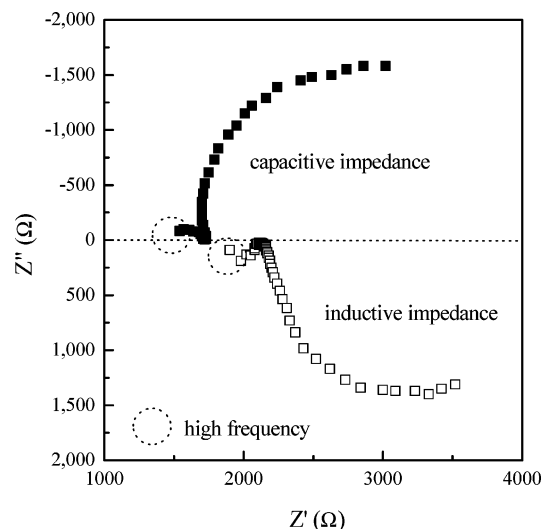


Figure 5. The Nyquist plot for Nafion 112 (■) derived from the four-probe method and for Nafion 112 (□) derived from the two-probe method in the frequency range from 100 kHz to 0.1 Hz at temperature 60 °C and 82% RH.

behavior in the Nyquist impedance plot. For the two-probe method, all Nyquist plots for membrane samples within the controlled temperature and humidity range showed positive reactance values. This indicated well that, in the two-probe method, the inductive impedance derived from BPO connectors, Pt electrodes, and leads including coaxial cables, except the ohmic resistance of the membrane sample, was more predominant than the capacitive impedance between the electrodes,²⁶ although the inductors components have relatively lower impedance in the overall impedance measurement system.

For the four-probe method, in contrast to the two-probe method, the inductive impedance can be ignored in the total impedance, because the current path and voltage-sensing cables are independent of each other.^{30–32} That is, only the capacitive reactance was considered in the total impedance, including the ohmic resistance. Typically, all Nyquist impedance plot in the four-probe method showed negative reactance values on the Z'' axis, reflecting the predominant capacitive impedance, and exhibited a semicircular arc and subsequently a rising curve similar to that of the typical Nyquist plot in Figure 4. The first semicircular arc is closely related to the complex impedance of the Nafion membranes and membrane-electrode interface, and the second rising curve is attributed to the Warburg impedance resulting from diffusion of water. The ohmic resistance in each membrane sample was obtained from the first approximation of the impedance obtained from the Nyquist plot, and the proton conductivity was derived from eq 4 using the ohmic resistance. Additionally, all Nyquist plots measured using the two-probe method and the

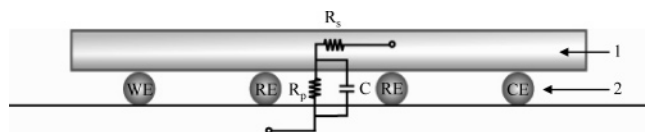


Figure 6. The equivalent circuit for the complex impedance of the Nafion membranes and the electrode structure: 1, proton-conductive Nafion membrane; 2, Pt electrodes on Teflon plate (WE, working electrode; CE, counter electrode; RE, reference electrode). In case of the two-probe cell, CE and WE coincide with two RE, respectively.

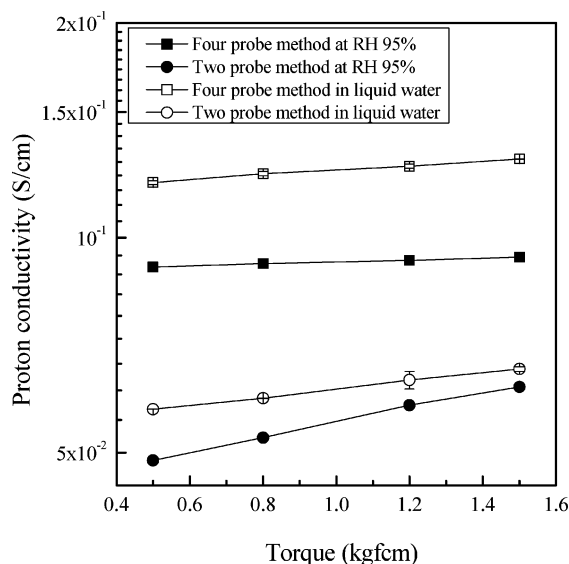


Figure 7. The proton conductivity as a function of torque applied to Nafion 112 by knurled nuts onto the four-probe electrodes (■) and the two-probe electrodes (●) in the water-vapor state at 95% RH and 60 °C and the four-probe electrodes (□) and the two-probe electrodes (○) in the liquid-water state at 60 °C.

four-probe method in liquid water showed only negative reactance, independent of inductive impedance. Figure 6 illustrated the equivalent circuit for the complex impedance of a Nafion membrane and the electrode structure. The ohmic resistance is connected in series with a parallel circuit consisting of the interface resistance and the capacitance between the reference electrodes.

As can be seen in Figure 7, the impedance and subsequent proton conductivity were measured as a function of torque (kgf·cm) applied to the membrane sample through the Teflon cover by screwing the knurled nuts. Higher torque leads to the reduction of contact resistance between the membrane sample and electrodes. The bulk resistance, which consists of the ohmic resistance; the contact resistance; and the resistance of the Pt electrodes decreased and the corresponding conductivity increased with lower contact resistance owing to the constant ohmic resistance and the resistance of the Pt electrodes. As a result, the proton conductivity was affected by contact resistance between the membrane sample and electrodes depending on different cell configurations and measuring conditions such as the liquid-water and water-vapor state. The proton conductivity increased continuously with increasing torque. In the water-vapor state, the proton conductivity in the two-probe method increased much faster compared with the four-probe method, because of its higher influence on the contact resistance between each electrode and the membrane sample. Furthermore, the proton conductivity measured using the two-probe

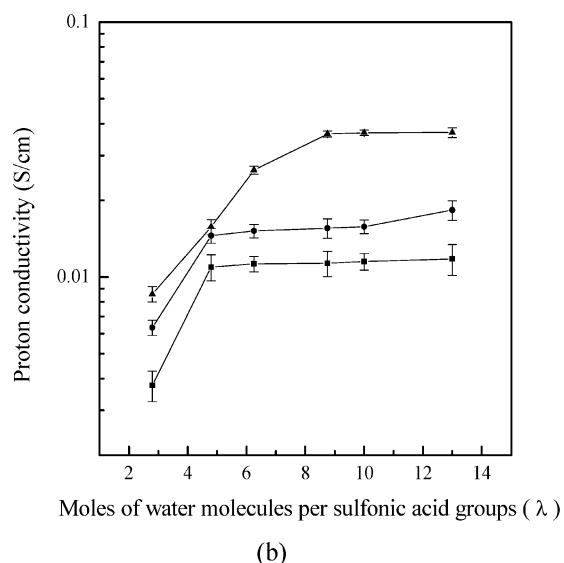
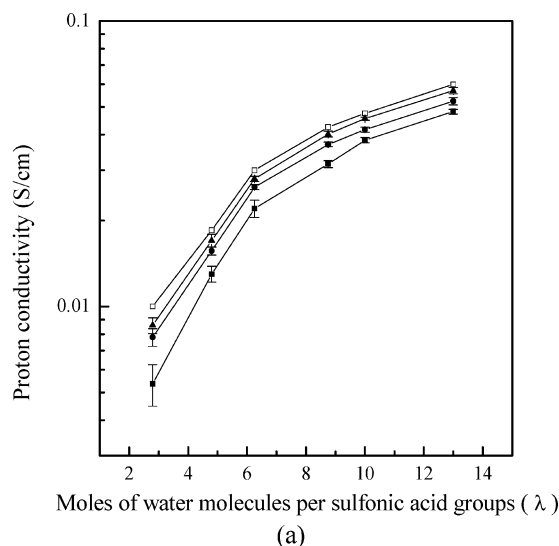


Figure 8. The proton conductivity of Nafion 117 (■), Nafion 115 (●), and Nafion 112 (▲) compared with that of Nafion 117 (□) reported by Zawodzinski et al.²³ as a function of water content in the membrane at 60 °C, using (a) the four-probe method and (b) the two-probe method.

method was lower than that for the four-probe method, because the coincidence of the current path and voltage sensing cable caused various errors, such as lead impedances in the pathway of a constant current flow as well as a contact resistance to a significant extent. The maintenance of water content in the membrane sample by controlling the relative humidity is not easy, even in a chamber with calibrated hygrometer and thermometer, while the constant water content is simply kept in liquid water. In the impedance measurement in liquid water, a similar increasing rate of proton conductivity was observed in the two different cell configurations as the influence of the contact resistance could be minimized in the membrane sample with constant water content. The proton conductivity measured by the four-probe method was higher than that measured by the two-probe method.

The relationship between the conductivity and the water content in a membrane is shown at 60 °C as a function of proton conductivity and λ in Figure 8. The λ value was solely affected by the water content in a membrane at a specific humidity condition, as the IEC

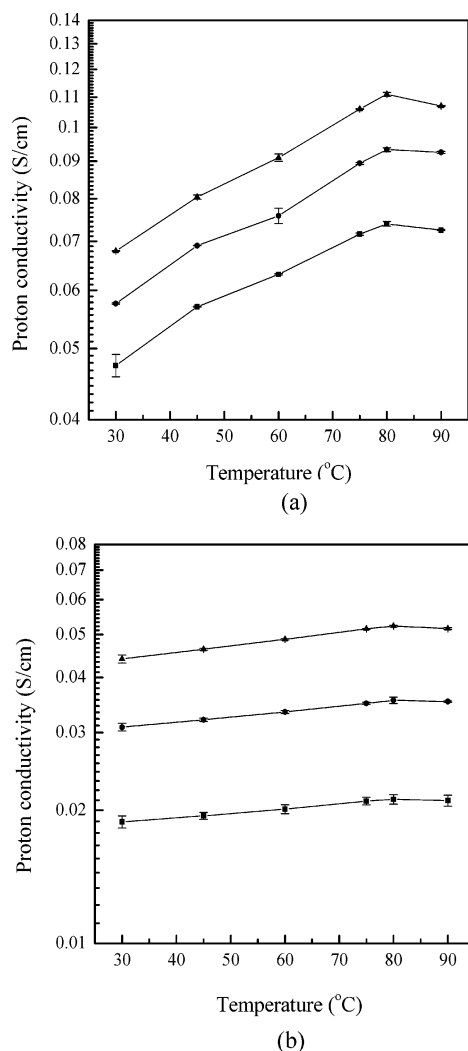


Figure 9. The proton conductivity of Nafion 117 (■), Nafion 115 (●), and Nafion 112 (▲) as a function of temperature at 95% RH using (a) the four-probe method and (b) the two-probe method.

was constant for the same membrane sample. The proton conductivity was measured not in water ($\lambda = 14$) but under water-vapor conditions, considering the usual PEMFC operating condition. The range of λ was from 2.8 mol of H_2O as the minimum water content to 13 mol of H_2O /mol of sulfonate group as the maximum water content, as the increase of the relative humidity caused higher water uptake in the membrane sample and a consequent increase of λ . Because the water content in the membrane significantly affects the proton transport via the Grötthaus hopping mechanism and vehicle mechanism, a higher proton conductivity was observed with an increase of λ . The proton conductivity of Nafion membranes, mainly Nafion 117, has been measured using several methods and reported differently by many research groups.^{8–22} The proton conductivity in Nafion 112, 115, and 117 derived from the four-probe method was almost consistent with that of Nafion 117 reported by Zawodzinski et al.²³ In addition, the unique behavior of Nafion membrane—that the proton conductivity increased relatively quickly at low water content in the membrane and then gradually at high water content because of high ion density clusters forming ion-rich channels³³—was also well shown in the measurement using the four-probe method. The proton conductivity of Nafion 112 was somewhat higher than those of the other membranes and the proton conductivity of Nafion

117 was a little lower than the others. It may be inferred that the nominal thickness of each membrane caused the difference in the proton conductivity, as a thicker membrane needed extra time to absorb water vapor to the fully hydrated state. In the two-probe method, it was shown that the proton conductivity of Nafion 112 was likely to be independent of the water content in the membrane at high humidity, whereas the proton transport behavior at relatively low and moderate humidity was similar to the typical behavior of Nafion. This unexpected, nonideal behavior in the proton transportation was observed clearly in thicker membranes at the same impedance measurement condition using the two-probe method.

The temperature dependence on the proton transport behavior for all perfluorinated membrane samples was observed using the two different cell configurations at 95% RH in Figure 9. The proton conductivity of Nafion 112, derived from the four-probe method, increased continuously up to about 0.11 S/cm at 80 °C. Although the proton conductivities of Nafion 115 and 117 were lower than that of Nafion 112 under the same measurement conditions, their conductivity increased at elevated temperature. Additionally, at around 80 °C, a drastic decrease in the proton conductivity of all Nafion membranes was observed because of the high vaporization rate of water from the Nafion membrane under this water-vapor condition. On the other hand, the proton conductivity obtained from the two-probe method reached about 0.05 S/cm for Nafion 112, although its proton conductivity also increased up to 80 °C and decreased again above this temperature. This phenomenon was less prominent in the case of thicker membranes such as Nafion 115 and 117.

Additionally, the electrochemical behavior of each membrane sample in liquid water was also observed using the different impedance measurement methods. Figure 10 shows that proton conductivity successively increased up to 90 °C even in different cell configurations. In the case of impedance measurement in liquid water, the continuous supply of liquid water maintained the constant water retention level within the membrane sample. That is, unlike the water-vapor state, the proton conductivity was not influenced by the effect of water desorption from the membrane. Figure 10 also shows a 2–5-fold difference in proton conductivity for Nafion membranes between the two-probe and four-probe methods. This difference in proton conductivity obtained from this study is in good agreement with the literature.^{34–36} The main reason for this difference in proton conductivity is that the impedance measured by the two-probe method includes various resistor components, such as leads, BPO connectors, and a potentiometer, as well as bulk resistance containing ohmic resistance, contact resistance, and resistance of electrodes, and these error sources cause the considerable reduction in proton conductivity and the inaccuracy in the measurement method.

The relationship between the temperature (T) and the proton conductivity (σ) measured using the four-probe method and the two-probe method was expressed well with the activation energy (E_a) for the proton conduction behavior of each perfluorinated membrane derived from the Arrhenius equation as described in eq 10.

$$\ln \sigma = \ln \sigma_0 - \frac{E_a}{RT} \quad (10)$$

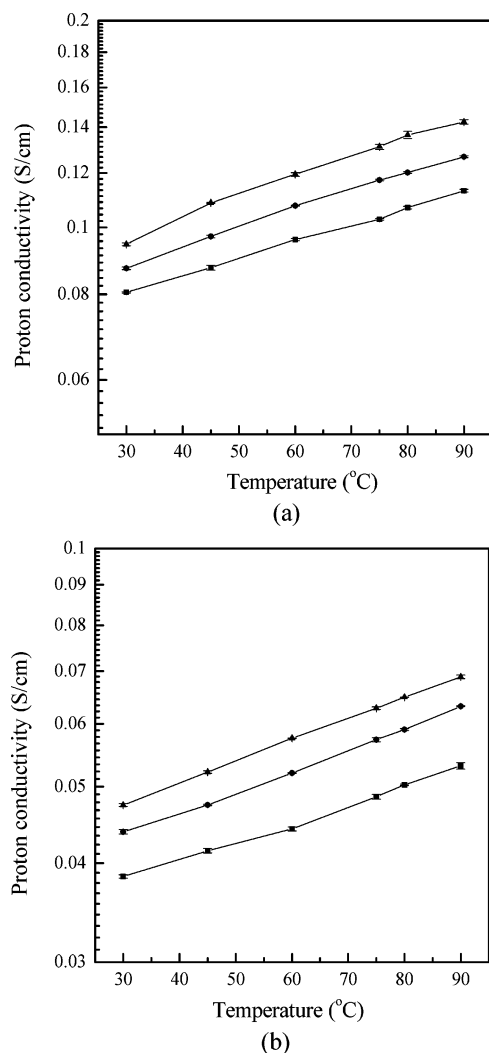


Figure 10. The proton conductivity of Nafion117 (■), Nafion 115 (●), and Nafion 112 (▲) as a function of temperature in liquid water using (a) the four-probe method and (b) the two-probe method.

where R is the gas constant, T is the absolute temperature, and σ_0 is independent of T as the frequency factor. For the proton conduction, it was found that each plot of $\ln \sigma$ against $1/T$ gave a straight line. The activation energy, which is the minimum energy required for proton conduction through each Nafion membrane, was obtained from the slope in the linear fit and is shown in Table 1. Generally, a high activation energy means that the proton conductivity changes rapidly with temperature. In the measurement using the four-probe method, the activation energies of Nafion membranes were within the range from 5.1 to 8.7 kJ/mol, which are similar to values from other studies.^{37–40} The obvious temperature dependence of proton conductivity was observed explicitly when the four-probe method was used. On the other hand, the activation energies derived from the two-probe method in the water-vapor condition were much lower than the reported activation energy of Nafion, and also the proton transport behavior of Nafion seemed to be independent of the temperature. However, the activation energies measured in the liquid-water state were within the range of the activation energies reported in the literature. As a result, the effect of temperature on the proton conductivity was not fully explained with the two-probe method under the water-vapor condition because of many error sources,

Table 1. Basic Properties and Activation Energies of Nafion Membranes Using Impedance Spectroscopy in the Water-Vapor State and the Liquid-Water State

sample	nominal thickness (μm)	basis weight (g/m^2)	activation energy (kJ/mol)	
			two-probe method	four-probe method
Nafion 117	170	360	21.0 ^{17,a}	9.71 ^{37,c}
			12.0 ^{17,b}	7.82 ^{38,d}
			2.12 ^g	13.4 ^{39,e}
			4.89 ^h	17.2 ^{40,f}
Nafion 115	127	250		7.46 ^g
			2.49 ^g	5.14 ^h
			5.58 ^h	8.40 ^g
Nafion 112	51	100		5.71 ^h
			3.08 ^g	8.65 ^g
			5.68 ^h	6.23 ^h

^a Measured in the temperature range from 30 to 40 °C and 100% RH over a frequency range from 1 Hz to 65 kHz. ^b Measured in the temperature range from 50 to 70 °C and 100% RH over a frequency range from 1 Hz to 65 kHz. ^c Measured in the temperature range from 25 to 90 °C by the current interruption method during the PEMFC single cell test. ^d Measured in the temperature range from 15 to 125 °C and liquid water using an ac bridge at 1000 Hz. ^e Measured in the temperature range from 20 to 90 °C over a frequency range from 1 Hz to 65 kHz. ^f Measured in the temperature range from 25 to 70 °C in liquid water over a frequency range from 10 Hz to 10 kHz. ^g Measured in this study in the temperature range from 30 to 90 °C and 95% RH over a frequency range from 0.1 Hz to 100 kHz. ^h Measured in this study in the temperature range from 30 to 90 °C in liquid water over a frequency range from 0.1 Hz to 100 kHz.

including the contact resistance and the lead impedance such as l_{lead} , r_{lead} , and C_{stray} causing the steep decrease of the characteristic proton conductivity in the membrane samples.

Comparing the impedance and the subsequent proton conductivity derived from the two-probe method and the four-probe method with Nafion membranes as standard samples in different measurement conditions (Figures 8–10), it was revealed that the four-probe method was more suitable and extensively applicable to measuring the inherent impedance and the specific proton conductivity of a membrane over a very wide range of both temperature and humidity, while the two-probe method was able to be used restrictively in a low humidity condition. Moreover, it was found that the proton conductivity derived from the two-probe method in both water vapor and liquid water is generally lower compared with the four-probe method, because the impedance in the two-probe method included the lead impedance containing the l_{lead} , r_{lead} , and C_{stray} as well as various resistances, such as the ohmic resistance of the membrane sample, contact resistance, and resistance of Pt electrodes.

In contrast to impedance measurement in proton exchange membranes, the two-probe method is not always an inappropriate and inaccurate method. As described above, the impedance measured using the two-probe method includes all impedance components in the pathway from the test sample to the potentiometer through the Pt electrodes. For this reason, the two-probe method can be applied to find critical reasons for reduction of fuel cell performances, measuring complex impedance in the overall fuel cell system. In summary, the two-probe method is suitable and applicable not for the measurement of the inherent impedance and subsequent proton conductivity of a membrane, but for the measurement of the complex impedance from fuel cell elements such as MEA, bipolar plate, end plate, and current collector as resistor, inductor, and capacitor.

Conclusions

A precise impedance measurement system was prepared to obtain the impedance and the consequent proton conductivity of a proton-exchange membrane via the four-probe method and the two-probe method using the autobalancing bridge method. The system was composed of the electrode systems with two different cell configurations connected with a Solatron 1287 in combination with a Solatron 1260, the base plate for electrical connection, and the thermo- and hygrocontrolled metallic chamber to ensure a more stable measurement without any electromagnetic noise. Three different kinds of Nafion membranes were selected and utilized as standard samples to measure and observe the proton transport behavior under various measuring conditions, such as different cell configurations and the thermo- and hygrocontrolled atmosphere. The impedance measurement was conducted, after each dried Nafion membrane was allowed to reach equilibrium water content. The impedance measurement in the water-vapor state for the same membrane led to different behaviors, where the inductive impedance in the two-probe method and the capacitive impedance in the four-probe method were predominant, respectively. The effect of contact resistance on proton conductivity was predominant in the impedance measurement in the water-vapor state using the two-probe method. The proton conductivity derived from approximation of the Nyquist impedance plot was close to the reported proton conductivity in the four-probe method. The proton transport behavior through the membrane over a wide range of humidity was much better observed by the four-probe method, whereas it was able to be restrictively observed at relatively low and moderate humidity. The temperature dependence of the proton transport was shown using the proton conductivity, and the activation energy of each membrane sample was determined over a temperature range from 30 to 90 °C. As all impedance components in the pathway of the current flow influenced the two-probe method, the proton conductivity derived from the two-probe method was much lower than that in the four-probe method and seemed to be independent of temperature. As a result, the four-probe method was applicable to the measurement of the inherent impedance and the subsequent proton conductivity of a membrane over a wide range of both humidity and temperature, whereas the two-probe method was appropriate for measuring total impedance of the electrochemical cell with the cell performance dependent on the resistances of all components as well as for the impedance measurement of a membrane in low humidity.

Acknowledgment

The authors thank the Ministry of Commerce, Industry and Energy for funding this research (M1042503000704L250300710). C.H.L. is grateful to the Brain Korea (BK) 21 Project for fellowship.

Literature Cited

- (1) Day, T. J. F.; Schmitt, U. W.; Voth, G. A. The mechanism of Hydrated Proton Transport in Water. *J. Am. Chem. Soc.* **2000**, *122*, 12027–12028.
- (2) Eikerling, M.; Kornyshev, A. A.; Kuznetsov, A. M.; Ulstrup, J.; Walbran, S. Mechanisms of Proton Conductance in Polymer Electrolyte Membranes. *J. Phys. Chem. B* **2001**, *105*, 3646–3662.
- (3) Spohr, E.; Commer, P.; Kornyshev, A. A. Enhancing Proton Mobility in Proton Exchange Membranes: Lessons from Molecular Dynamics Simulations. *J. Phys. Chem. B* **2002**, *106*, 10560–10569.
- (4) Kornyshev, A. A.; Kuznetsov, A. M.; Spohr, E.; Ulstrup, J. Kinetics of Proton Transport in Water. *J. Phys. Chem. B* **2003**, *107*, 3351–3366.
- (5) Won, J. O.; Park, H. Y.; Kim, Y. J.; Choi, S. W.; Ha, H. Y.; Oh, I. H.; K, H. S.; Kang, Y. S.; Ihn, K. J. Fixation of Nanosized Proton Transport Channels in Membranes. *Macromolecules* **2003**, *36*, 3228.
- (6) Li, T.; Wlaschin, A.; Balbuena, P. B. Theoretical Studies of Proton Transport in Water and Model Polymer Electrolyte Systems. *Ind. Eng. Chem. Res.* **2001**, *40*, 4789–4800.
- (7) Kim, Y. S.; Dong, L.; Hickner, M. A.; Glass, T. E.; Webb, V.; McGrath, J. E. State of Water in Disulfonated Poly(arylene ether sulfone) Copolymers and a Perfluorosulfonic Acid Copolymer (Nafion) and Its Effect on Physical and Electrochemical Properties. *Macromolecules* **2003**, *36*(17) 6282–6285.
- (8) Hasiotis, C.; Deimede, V.; Kontoyannis, C. New Polymer Electrolytes Based on Blends of Sulfonated Polysulfones with Polybenzimidazole. *Electrochim. Acta* **2001**, *46*, 2401–2406.
- (9) Wilhelm, F. G.; Pünt, I. G. M.; Van der Vegt, N. F. A.; Strathmann, H.; Wessling, M. Cation Permeable Membranes from Blends of Sulfonated Poly(ether ether ketone) and Poly(ether sulfone). *J. Membr. Sci.* **2002**, *199*, 167–176.
- (10) Wang, F.; Hickner, M.; Ji, Q.; Harrison, W.; Mecham, J.; Zawodzinski, T. A.; McGrath, J. E. Synthesis of Highly Sulfonated Poly(arylene ether sulfone) Random (statistical) Copolymers via Direct Polymerization. *Macromol. Symp.* **2001**, *175*, 387–396.
- (11) Hofmann, M. A.; Ambler, C. M.; Maher, A. E.; Chalkova, E.; Zhou, X.; Lvov, X. Y.; Allcock, H. R. Synthesis of Polyphosphazenes with Sulfoimide Side Groups. *Macromolecules* **2002**, *35*, 6490–6493.
- (12) Hommura, S.; Kunisa, Y.; Terada, I.; Yoshitake, M. Characterization of Fabril Reinforced Membranes for Fuel Cells. *J. Fluorine Chem.* **2003**, *5880*, 1–5.
- (13) Zhou, X.; Weston, J.; Chalkova, E.; Hofmann, M. A.; Ambler, C. M.; Allcock, H. R.; Lvov, S. N. High-Temperature Transport Properties of Polyphosphazene Membranes for Direct Methanol Fuel Cell. *Electrochim. Acta* **2003**, *48*, 2173–2180.
- (14) Fang, J.; Guo, X.; Harada, S.; Watari, T.; Tanaka, K.; Kita, H.; Okamoto, K. Novel Sulfonated Polyimides as Polyelectrolytes for Fuel Cell Application. 1. Synthesis, Proton Conductivity, and Water Stability of Polyimides from 4,4'-Diaminodiphenyl Ether-2,2'-disulfonic Acid. *Macromolecules* **2002**, *35*, 9022–9028.
- (15) Guo, X.; Fang, J.; Watari, T.; Tanaka, K.; Kita, H.; Okamoto, K. Novel Sulfonated Polyimides as Polyelectrolytes for Fuel Cell Application. 2. Synthesis and Proton Conductivity of Polyimides from 9,9-Bis(4-aminophenyl)fluorine-2,7-disulfonic Acid. *Macromolecules* **2002**, *35*, 6707–6713.
- (16) Yin, Y.; Fang, J.; Cui, Y.; Tanaka, K.; Kita, H.; Okamoto, K. Synthesis, Proton Conductivity and Methanol Permeability of a Novel Sulfonated Polyimide from 3-(2',4'-diaminophenoxy)propane Sulfonic Acid. *Polymer* **2003**, *44*, 4509–4518.
- (17) Piek, P. C.; Vanderborgh, N. E. Temperature Dependence of Water Content and Proton Conductivity in Perfluorosulfonic Acid Membranes. *J. Membr. Sci.* **1987**, *32*, 313–328.
- (18) Hong, L.; Zhou, Y.; Chen, N.; Li, K. Association of Nafion with Polypyrrole Nanoparticles in a Hydrophilic Polymer Network: Effect on Proton Transport. *J. Colloid Interface Sci.* **1999**, *218*, 233–242.
- (19) Kawahara, M.; Morita, J.; Rikukawa, M.; Sanui, K.; Ogata, N. Synthesis of Proton Conductivity of Thermal Stable Polymer Electrolyte: Poly(benzimidazole) Complexes with Strong Acid Molecules. *Electrochim. Acta* **2000**, *45*, 1395–1398.
- (20) Zaidi, S. M. J.; Mikhailenko, S. D.; Robertson, G. P.; Guiver, M. D.; Kaliaguine, S. Proton Conducting Composite Membranes from Polyether Ether Ketone and Heteropolyacids for Fuel Cell Application. *J. Membr. Sci.* **2000**, *173*, 17–34.
- (21) Staiti, P.; Lufrano, F.; Aricò, A. S.; Passalacqua, E.; Antonucci, V. Sulfonated Polybenzimidazole Membranes—Preparation and Physicochemical Characterization. *J. Membr. Sci.* **2001**, *188*, 71–78.
- (22) Glipa, X.; Haddad, M. E.; Jones, D. J.; Rozière, Synthesis and Characterisation of Sulfonated Polybenzimidazole: A Highly Conducting Proton Exchange Polymer. *J. Solid State Ionics* **1997**, *97*, 323–331.

- (23) Zawodzinski, T. A.; Neeman, M.; Sillerud, L. O.; Gottesfeld, S. Determination of Water Diffusion Coefficient in Perfluorosulfonate Ionomeric Membranes. *J. Phys. Chem.* **1991**, *95*, 6040–6044.
- (24) Oldham, K. B.; Myland, J. C. *Fundamentals of Electrochemical Science*; Academic Press: New York, 1994.
- (25) Scaife, B. K. P. *Principles of Dielectrics*; Clarendon Press: Oxford, 1989.
- (26) Honda, M. *The Impedance Measurement Handbook—A Guide to Measurement Technology and Techniques*; Yokogawa-Hewlett-Packard Ltd.: Tokyo, 1989.
- (27) Greenspan, L. Functional Equations for the Enhancement Factors for Carbon Dioxide-free Moist Air. *J. Res. Natl. Bur. Stand.* **1976**, *80*(1), 41–44.
- (28) LaConti, A.; Fragala, A.; Boyack, J. In *Electrode Materials and Processes for Energy Conversion and Storage*; McIntyre, J. D. E., Srinivasan, S., Will, F., Eds.; The Electrochemical Society: Penninton, NJ, 1977; p 354.
- (29) Bruce, P. G.; West, A. R. The AC Conductivity of Polycrystalline LISICON, Lithium Zinc Germanate ($\text{Li}_2+2\text{xZn}1-\text{xGeO}_4$), and a Model for Intergranular Constriction Resistances. *J. Elec. Chem. Soc.* **1983**, *130*(3), 662–669.
- (30) Cutkosky, R. D. Four-Terminal-Pair Network as Precision Admittance and Impedance Standards. *Trans. IEEE Commun. Electron.* **1964**, *83*, 19–22.
- (31) Shield, J. Q. Measurement of Four-pair Admittances with Two-Pair Bridges. *Trans. IEEE Instrum. Meas.* **1974**, *23*, 345–352.
- (32) Kibble, B. P.; Rayner, G. H. *Coaxial Bridges*; Adam Hilger Ltd: Bristol, 1983; pp 18–25.
- (33) Gierke, T. D.; Munn, G. E.; Wilson, F. C. The Morphology in Nafion Perfluorinated Membrane Products, as Determined by Wide- and Small-Angle X-ray Studies. *J. Polym. Sci. Polym. Phys. Ed.* **1981**, *19*, 1687–1704.
- (34) Gardner, C. L.; Anantaraman, A. V. Measurement of Membrane Conductivities Using an Open-Ended Coaxial Probe. *J. Electroanal. Chem.* **1995**, *395*, 67–73.
- (35) Tricoli, V.; Carretta, N.; Bartolozzi, M. A. Comparative Investigation of Proton and Methanol Transport in Fluorinated Ionomeric Membranes. *J. Electrochem. Soc.* **2000**, *147*, 1286–1290.
- (36) Elabd, Y. A.; Walker, C. W.; Beyer, F. L. Triblock Copolymer Ionomer Membranes Part. II. Structure Characterization and Its Effects on Transport Properties and Direct Methanol Fuel Cell Performance. *J. Membr. Sci.* **2004**, *231*, 181–188.
- (37) Lufrano, F.; Gatto, I.; Staiti, P.; Antonucci, V.; Passalacqua, E. Sulfonated Polysulfone Ionomer Membranes for Fuel Cells. *Solid State Ionics* **2001**, *145*, 47–51.
- (38) Kopitzke, R. W.; Linkous, C. A.; Anderson, H. R.; Nelson, G. L. Conductivity and Water Uptake of Aromatic-based Proton Exchange Membrane Electrolytes. *J. Electrochem. Soc.* **2000**, *147*, 1677–1681.
- (39) Halim, J.; Büchi, F. N.; Haas, O.; Stamm, M.; Scherer, G. G. Characterization of Perfluorosulfonic Acid Membranes by Conductivity Measurements and Small-Angle X-ray Scattering. *Electrochim. Acta* **1994**, *39*, 1303–1307.
- (40) Doyle, M.; Lewittes, M. E.; Roelofs, M. G.; Perusich, I. Ionic Conductivity of Nonaqueous Solvent-Swollen Ionomer Membrane Based on Fluorosulfonate, Fluorocarboxylate, and Sulfonate Fixed Ion Groups. *J. Phys. Chem. B* **2001**, *105*, 9387–9394.

Received for review January 31, 2005

Revised manuscript received April 19, 2005

Accepted April 20, 2005

IE0501172